

Article

Effect of Valve Timing and Excess Air Ratio on Torque in Hydrogen-Fueled Internal Combustion Engine for UAV

Cheolwoong Park ^{1,*} , Wonah Park ¹, Yongrae Kim ¹, Young Choi ¹ and Byeungjun Lim ²

¹ Engine Research Team, Environmental System Research Division, Korea Institute of Machinery and Materials, Daejeon 34103, Korea; wpark@kimm.re.kr (W.P.); yrkim@kimm.re.kr (Y.K.); ychoi@kimm.re.kr (Y.C.)

² Engine Component Technology Team, Aeropropulsion Division, Korea Aerospace Research Institute, Daejeon 34133, Korea; bjl@kari.ac.kr

* Correspondence: cwpark@kimm.re.kr; Tel.: +82-42-868-7928

Received: 18 December 2018; Accepted: 20 February 2019; Published: 26 February 2019



Abstract: In this study, in order to convert a 2.4 L reciprocating gasoline engine into a hydrogen engine an experimental device for supplying hydrogen fuel was installed. Additionally, an injector that is capable of supplying the hydrogen fuel was installed. The basic combustion characteristics, including torque, were investigated by driving the engine with a universal engine control unit. To achieve stable combustion and maximize output, the intake and exhaust valve opening times were changed and the excess air ratio of the mixture was controlled. The changes in the torque, excess air ratio, hydrogen fuel, and intake airflow rate, were compared under low engine speed and high load (wide open throttle) operating conditions without throttling. As the intake valve opening time advanced at a certain excess air ratio, the intake air amount and torque increased. When the opening time of the exhaust valve was retarded, the intake airflow rate and torque decreased. The torque and thermal efficiency decreased when the opening time of the intake and exhaust valve advanced excessively. The change of the mixture condition's excess air ratio did not influence the tendency of the torque variation when the exhaust valve opening time and torque increased, and when the mixture became richer and the intake valve opening time was fixed. Under a condition that was more retarded than the 332 CAD condition, the torque decreased by about 2 Nm with the 5 CAD of intake valve opening time retards. The maximum torque of 138.1 Nm was obtained at an optimized intake and the exhaust valve opening time was 327 crank angle degree (CAD) and 161 CAD, respectively, when the excess air ratio was 1.14 and the backfire was suppressed. Backfire occurred because of the temperature increase in the combustion chamber rather than because of the change in the fuel distribution under the rich mixture condition, where the other combustion control factors were constantly fixed from a three-dimensional (3D) computational fluid dynamics (CFD) code simulation.

Keywords: hydrogen; port fuel injection engine; torque; backfire; excess air ratio; valve opening time

1. Introduction

Recently, interest in unmanned devices has been steadily growing in the aviation industry, and the demand for the research and development of unmanned aerial vehicles (UAVs) for communications and reconnaissance has been increasing. The development of high-altitude, long-endurance UAVs that are suitable to reconnaissance and telecommunication operations, while maintaining a high altitude for a long period of time, is also included in this category [1,2]. One of the most important technologies to be developed is the power source technology for UAVs. The use of high-energy-density fuels is essential for long-term storage at high altitude, and liquid hydrogen is the most promising among

these fuels. The energy density of hydrogen fuel, which is approximately 120 MJ/kg [3], is much higher than that of conventional hydrocarbon series liquid fuels, which is approximately 45 MJ/kg. Moreover, hydrogen fuel does not contain carbon, which makes it valuable as a clean fuel, since it does not produce greenhouse gas emissions.

Hydrogen has been widely identified as an explosive fuel and it requires handling because its flammability limit is very broad and its ignition energy is very low. However, in recent years, owing to the importance of renewable energy and the emergence of new energy technologies, such as fuel cells, hydrogen fuel has become the focus of many studies due to its potential to provide a means of securing the economic efficiency of the entire hydrogen-powered system by hydrogen production and storage, despite of the safety issues that are entailed in the use of hydrogen fuel [4]. However, in order to apply hydrogen fuel to existing combustion equipment, it is still necessary to overcome technical combustion problems that result from the high reactivity of hydrogen. Research and development activities have been conducted within various fields in order to address these problems [5–10].

In particular, various research groups have carried out research and development with regard to applying hydrogen fuel to automotive engines for a long time. Such activities have ranged from spark ignition engines and favoring gas engines to premixed compression ignition combustion [11–13]. The German company BMW has developed a vehicle that uses hydrogen as fuel since the 1970s [14]. The American company Ford has also developed a hydrogen engine by converting its conventional gasoline engine [15]. However, Ford has not yet commercialized this technology. Various relevant studies have been conducted in Korea; however, they are still in the level of basic research, owing to various environmental constraints.

Although hydrogen engines directly supplying hydrogen gas to the cylinder have been investigated, the mixing ratio of hydrogen and air is relatively reduced when compared with the port injection so that the thermal efficiency can be reduced because of the direct injection of the gaseous fuel during the compression process. Moreover, there are a lot of problems with regard to practical implementation, since the reliability and air-tightness of the high-pressure injectors must be secured [16]. Therefore, the intake port injection type hydrogen engine with high thermal efficiency is advantageous because of the increase of the hydrogen's mixing period and air. Additionally, the fuel system of an existing gasoline or natural gas engine can be easily converted. However, the intake port injection system has a disadvantage, which consists of the occurrence of backfire in the high load operating region. The cause of backfire has not yet been clarified; however, it is thought that premature ignition occurs because there exists a kind of ignition source in the combustion chamber, which is caused by the flame back-flowing into the intake pipe due to the rapid burning rate of hydrogen [17].

In the case of a high altitude long-endurance (HALE) UAV, on which this study focused, it was assessed that hydrogen with the highest energy density is the most appropriate and practical type of fuel. Since HALE UAV does not require fast flight speed, an internal combustion engine with high thermal efficiency is suitable and using hydrogen with a high energy density can solve the problem of restriction of the flying time due to the fuel amount limitation. Moreover, hydrogen is used with a reciprocating internal combustion engine as the power source in order to ensure technical stability and to reduce the financial cost. In this study, we propose a hydrogen fuel system in order to reciprocate the internal combustion engines and the control of the fuel and air amount during the combustion is very important. The theoretical air amount (weight of air) required for the complete combustion of fuel is defined as the stoichiometric air-to-fuel ratio (34:1 for hydrogen) of the fuel, and the excess air ratio is calculated from the actual amount of excess air for the combustion compared to the theoretical air amount of stoichiometric mixture. We selected a base engine that met the basic requirements, such as the size and weight of the target UAV, injector, and engine control unit (ECU). In particular, we aimed to achieve a stable combustion and maximize the output by changing the intake and exhaust valve opening time, and controlling the excess air ratio of the mixture in order to suppress the backfire, causing a decrease of output to the hydrogen engine of the intake port injection system. A simulation study with three-dimensional (3D) computational fluid dynamics (CFD) code was conducted in order

to predict the effect of the excess air ratio on the fuel and temperature distributions under the optimized intake conditions and exhaust valve openings.

2. Experimental Procedure

2.1. Experimental Setup

In order to realize the required performance of the UAV, we selected a 2.4 L gasoline engine with an intake port injection system that could produce a power output with a horsepower of at least 150, in addition to the capability of easily supplying the hydrogen fuel. Table 1 shows the specifications for the gasoline fuel base engine. Basically, the engine was installed in connection with the engine dynamometer, and the system was configured by using a general-purpose ECU (M800, Motec) for engine control, such as injection quantity and ignition timing.

Table 1. Engine specifications.

Engine Type	Gasoline (base)/Hydrogen–Naturally Aspirated
Number of cylinders	4
Bore × Stroke	88 mm × 97 mm
Displacement volume	2359 cc
Compression ratio	10.5
Maximum power output	131 kW at 6000 rpm
Maximum torque	228.5 Nm at 4000 rpm

The system configuration for supplying the hydrogen fuel to the engine was stored in a series of hydrogen tanks with a reservoir pressure of 10 MPa at a certain clearance distance from the laboratory, according to the gas safety law, and it was introduced in the laboratory through a hydrogen fuel line. The hydrogen fuel was supplied to the engine through depressurization by the regulator. The pure hydrogen was used in the test and the properties of hydrogen are compared to those of conventional gasoline in Korea in Table 2. The hydrogen flow rate was measured using a Coriolis type mass flow meter (CMF025M, Micromotion) and the thermal mass flowsensor (S452-80, CSi-TEC) was installed upstream of the intake manifold to measure the airflow rate in the test. Table 3 summarizes the specifications of each flow and torque measurement equipment.

Table 2. Properties of hydrogen and conventional gasoline fuels [18].

Fuel	Hydrogen	Gasoline
Octane number [-]	130+	90
Density at 1 atm and 300 K [kg/m ³]	0.082	707.1
Lower heating value [MJ/kg]	119.7	42.885
10% distillation temperature [dec C]	-	42.2
50% distillation temperature [dec C]	-	74.1
90% distillation temperature [dec C]	-	147.6

Table 3. Specifications of each flow and torque measurement equipment.

Parameter and Analyzer	Measuring Range	Accuracy	Uncertainty
Load cell for torque	0–1200 Nm	±0.2% of full scale	±1.4 Nm (about 95% confidence level, k = 2)
Hydrogen flow rate	0–240 kg/h	±0.25 of measured value	± 0.2 kg/h (about 95% confidence level, k = 2)
Airflow rate	6.7–1685.9 kg/h	±0.3 of full scale	± 2.9 kg/h (about 95% confidence level, k = 2)

The injectors at the intake manifold for each engine cylinder were replaced with a gas fuel injector at the same position as the existing gasoline fuel injector. Since a fully commercialized injector (high-pressure injectors for direct injection of hydrogen, HOERBIGER ValveTec GmbH) for hydrogen fuel is not commercially produced anymore, at the time of the experiment, a natural gas injector (NGI2, Bosch) for a passenger car engine was used. This gas injector could operate at an injection pressure of approximately 0.7 MPa. The leakage was always checked before and after the experiment, since there was a possibility of leakage when the long contact with the hydrogen fuel continued. Figure 1 shows a schematic diagram of the engine setup and the control/data acquisition system. A hydrogen leak detector and an automatic gas pipe shutoff valve were installed in preparation of hydrogen fuel leaks.

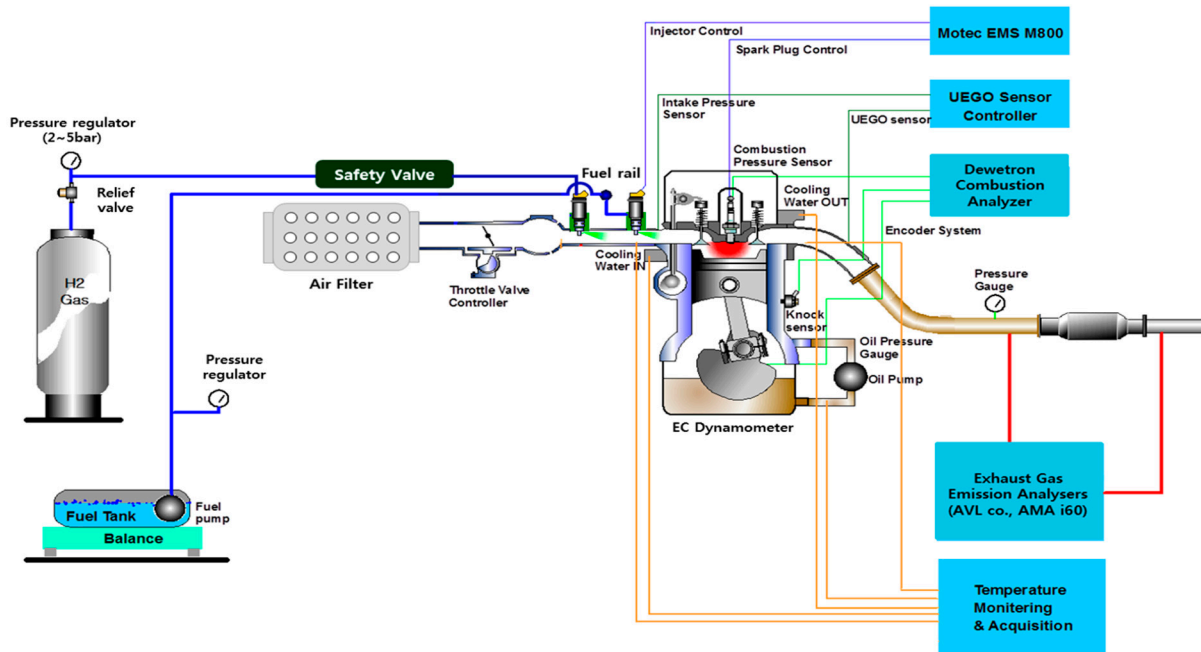


Figure 1. Schematic diagram of experimental setup.

$$\text{Brake thermal efficiency} = \text{Brake power} / \text{Fuel energy} = \frac{\text{Brake power [kW]} \times 3600}{\text{Fuel flow rate} \left[\frac{\text{kg}}{\text{hr}} \right] \times \text{Calorific value} \left[\frac{\text{kJ}}{\text{kg}} \right]} \times 100 \quad (1)$$

The equation of brake thermal efficiency is presented [19]. The brake thermal efficiency of the engine is defined as the ratio between the work output of the engine, which is brake power, and the lower heating value of the hydrogen fuel input. Temperature and pressure sensors were installed in order to receive the various temperatures and pressure data of the main engine parts in real-time under each engine operating condition. In particular, the spark plug integrated in-cylinder pressure sensor (6118BFD35, Kistler) was installed, and data, such as the combustion pressure and combustion stability, as represented by the coefficient of variation (COV) for the indicated mean effective pressure (IMEP) [19,20], were calculated through a combustion analyzer (DEWE-800-CA, Dewetron) based on the in-cylinder pressure data synchronized with the encoder. The excess air ratio was measured with a wide band oxygen sensor (LSU 4.2, Bosch) and lambda meter (LA4, ETAS).

2.2. Experimental Conditions

In the present study, we investigated the combustion characteristics of a conventional gasoline engine by using hydrogen fuel. First, the combustion stability was secured under the condition of 2000 rpm/wide open throttle (WOT), which corresponded to low speed and high load operating

conditions. Additionally, the effect of the excess air ratio and the opening time of the intake and exhaust valve on the combustion performance were assessed.

In Figure 2, the change in the torque, excess air ratio, hydrogen fuel, and intake airflow rate slightly decreases correspondingly with the gradual increase in hydrogen fuel, since the total amount of hydrogen/air mixture flow rate does not change under the WOT condition without throttling, and when the flow rate of the hydrogen fuel gradually increased in order to increase the output. Subsequently, the excess air ratio was reduced. However, if the excess air ratio decreased below a certain value, then backfire occurred and the torque sharply decreased. Backfire is a phenomenon by which the hydrogen-air mixture in the intake manifold is burned, when the supply of the hydrogen fuel is continuous and when the flow rate of the air into the intake manifold and the flow rate of the mixture to be supplied into the cylinder is instantly reduced because of the expansion of the combustion gas [21,22]. Consequently, a steady operation cannot be performed because of the sudden torque fluctuation when the hydrogen/air mixture is close to the stoichiometric condition, as shown in Figure 2. Therefore, in this study, to prevent the backfire the experiment was conducted from 1.3 of the initial excess air ratio of mixture, which is a relatively leaner mixture condition, and the amount of hydrogen increased to make the mixture become richer with an excess air ratio interval of 0.5.

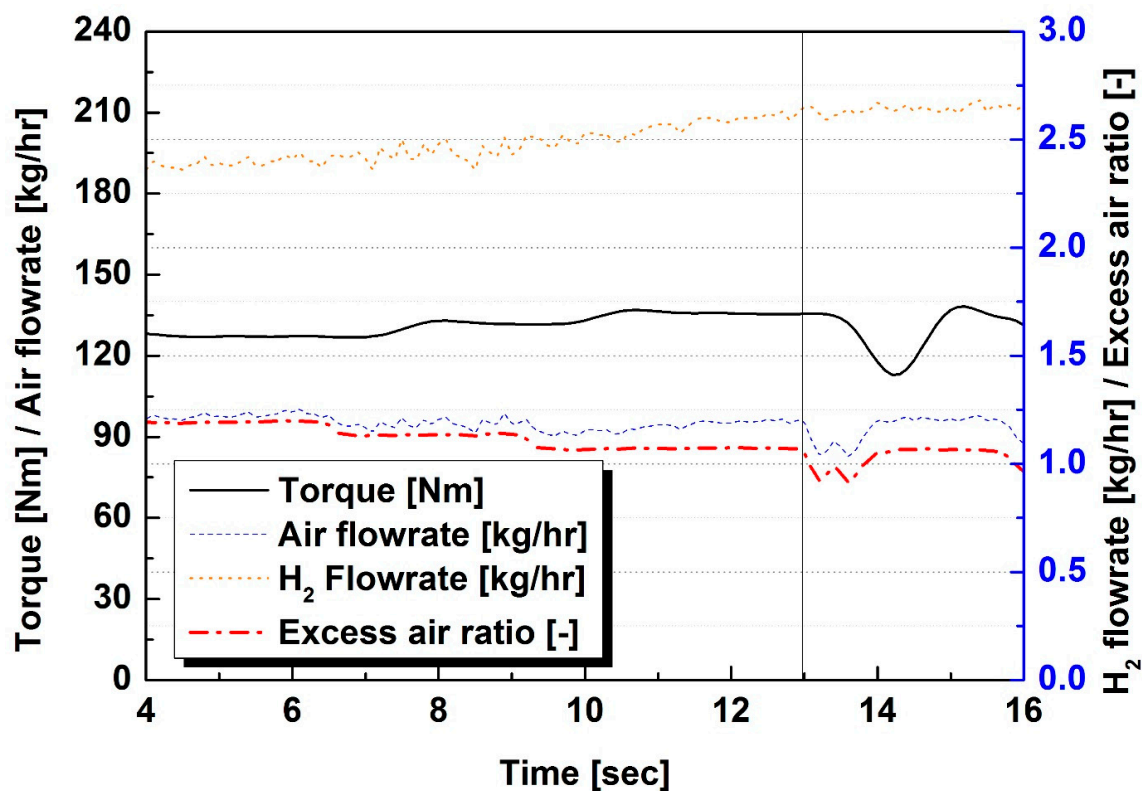


Figure 2. Torque, airflow, hydrogen flow, and excess air ratio changes in time with gradual increase in hydrogen fuel input.

The engine that was used in this study was equipped with a dual continuous variable valve timing function. The opening time of the intake valve could be advanced from a 367 crank angle degree (CAD) to a 322 CAD based on the after top dead center (ATDC). Additionally, the exhaust valve opening period could be retarded from 136 CAD to 176 CAD. If the opening time of the intake and exhaust valves was excessively advanced or retarded, then this would affect the backfire under the condition of a certain excess air ratio. Therefore, the experiments were conducted under stable operation points without backfire, and each valve opening timing was controlled with five CAD intervals, respectively.

In the last part, we compared the temperature and fuel distribution according to the change of the air-fuel mixer under optimal control conditions by using the STAR-CD 3D CFD (Computational Fluid Dynamics) code, in order to predict the cause of the backfire under the rich mix condition. The three-dimensional (3D) geometric model of the engine is obtained from the initial geometry data for the elements, such as part of the intake manifold, the cylinder head, cylinder, and piston. Computations were performed using the commercial CFD software, Star-CD ver. 4.26. The $k-\epsilon$ RNG (Re-Normalisation Group) model was used for the turbulence calculation [23,24]. Flow simulations were performed from IVO to TDC (Top Dead Center). The mesh includes approximately 1,138,000 cells at BDC (Bottom Dead Center) and the grid size is about 1 mm.

3. Results

First, the change of the torque and efficiency according to the change of the ignition time at the excess air ratios of 1.3 and 1.25 was investigated under the condition by which the opening time of the intake valve and the exhaust valve were fixed. As mentioned above, because of the WOT condition without throttling, the flow rate of the total amount of hydrogen and the air mixture did not change, while the excess air ratio changed as the supplied hydrogen fuel flow rate changed. The maximum brake thermal efficiency is shown in Figure 3, where it can be seen that, at the excess air ratio of 1.3, the torque was the highest at the spark advance time of five CAD before the top dead center (BTDC). However, at the excess air ratio of 1.25, which is a relatively richer mixture condition, the maximum efficiency and torque could be observed at three CAD BTDC, which is maximum brake torque (MBT) spark advance time. Although the burning rate is slightly slower in the relatively leaner mixture condition, as shown in Figure 4, it shows higher thermal efficiency because of higher air utilization rate and lower heat loss proportional to the combustion temperature. [18,25].

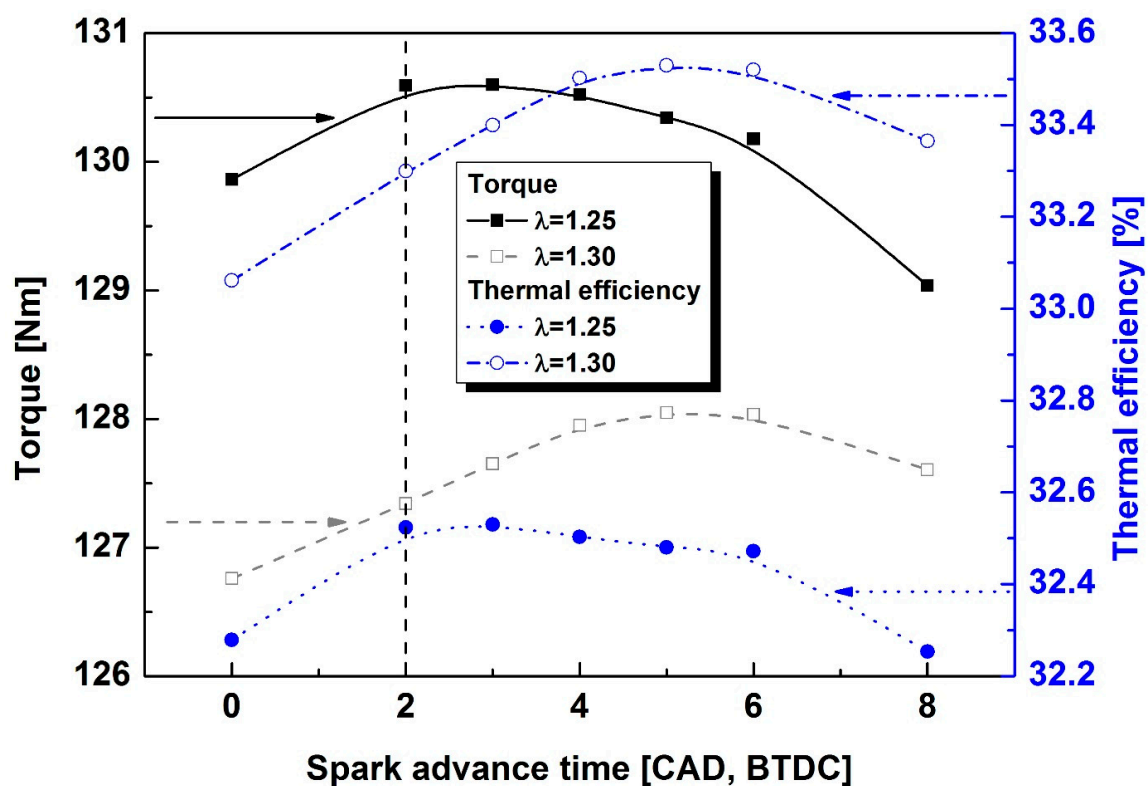


Figure 3. Torque and thermal efficiency variations with spark advance time changes at excess air ratios of 1.25 and 1.30.

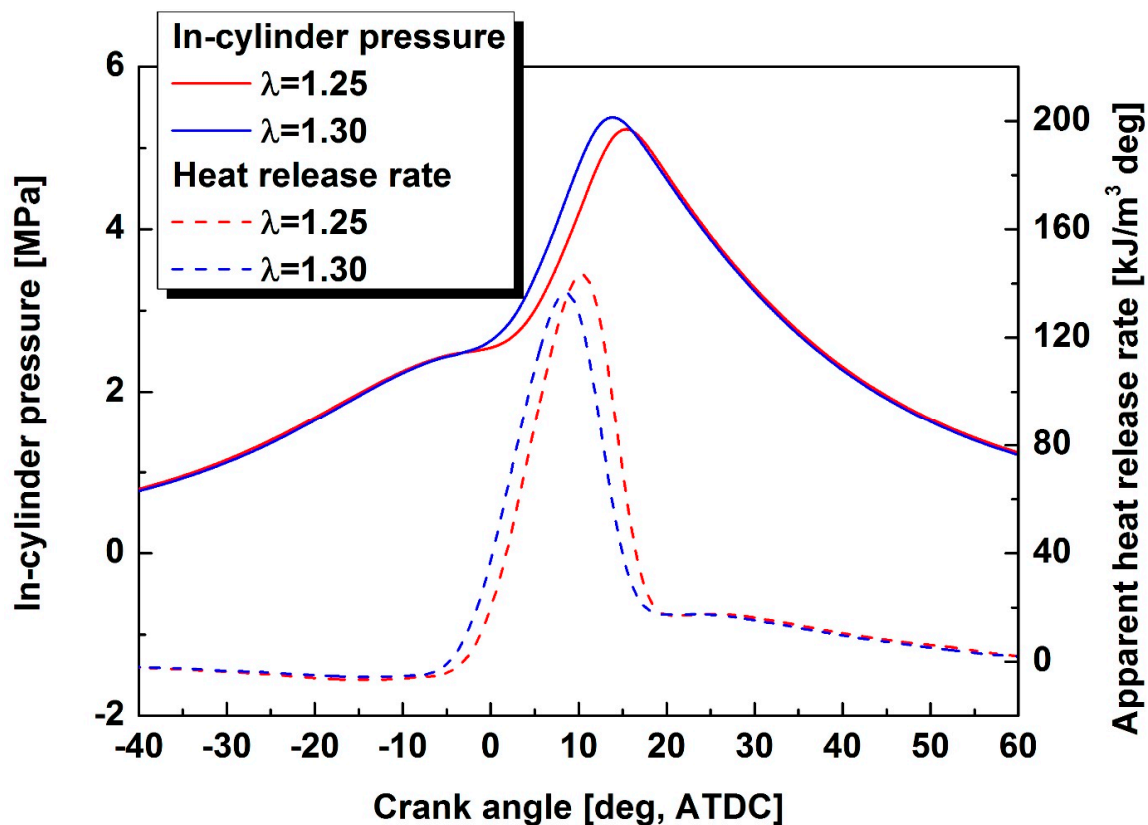


Figure 4. In-cylinder pressure and apparent heat release rate traces with maximum brake torque (MBT) spark advance time at excess air ratios of 1.25 and 1.30.

The influence of changing the valve opening time at the excess air ratio of 1.25, which can stably obtain higher torque, was investigated. Figure 5 describes the changes in torque, intake airflow rate, and efficiency when the opening time of the exhaust valve was fixed at 161 CAD ATDC with an excess air ratio of 1.25, and as the opening time of the intake valve changed. The opening and closing time of the intake valve affects the performance of the engine in relation to the volumetric efficiency, which represents the mass of the actual air that is introduced into the cylinder equivalent to the piston displacement. It is general, to advance the opening timing to a BTDC point so that as much intake air as possible can be introduced, since the flow rate of the intake air is not fast at low engine speed [26,27].

As can be seen in Figure 5, when the opening time advanced at a certain excess air ratio, the intake air amount in kg/h and torque increased. However, when the intake valve opened too soon, as was the case under the opening time condition of the 322 CAD ATDC, the intake airflow was reduced, because the exhaust gas obstructed it. Moreover, the closing time of the intake valve was too quick, since it occurred before the intake air was sufficiently introduced. Since the opening time was retarded, it was difficult to use the negative pressure generated when the exhaust gas was exhausted. Therefore, the flow rate of the intake air and the torque decreased. The flow rate of the intake air and the hydrogen fuel changed according to the change of the opening time. However, the efficiency was not significantly influenced, because the excess air ratio was maintained constant at 1.25. Moreover, if the opening time was excessively retarded under a certain exhaust valve opening time condition, even after the exhaust gas was fully exhausted, the intake valve would not be fully opened. This resulted in negative pressure, while the pumping loss was increased and it resulted in the reduction of torque. Since it is hard to measure the residual gas as evidence of internal EGR or rebreathing process by sampling the exhaust gas during the valve overlap, the simulation results of residual gas fraction changes are used to correlate the torque results in the cylinder for each intake and exhaust valve timing at the excess

air ratio of 1.25 with commercial one-dimensional (1D) simulation software (WAVE, Ricardo Inc.) as presented in Table 4.

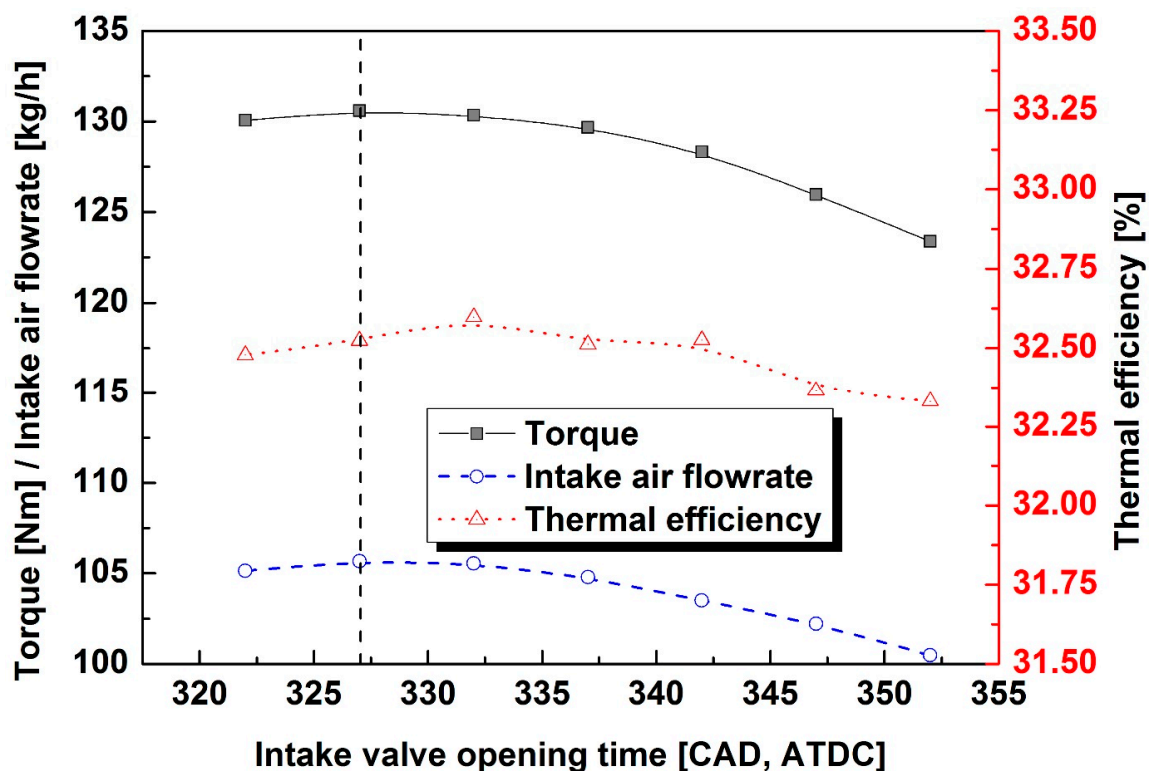


Figure 5. Torque, intake airflow rate, and thermal efficiency variations with intake valve opening time change at constant exhaust valve opening time of 161 CAD ATDC and excess air ratio of 1.25.

Table 4. Simulation results of residual gas fraction changes for each intake and exhaust valve timing at the excess air ratio of 1.25 with commercial one-dimensional (1D) simulation software (WAVE, Ricardo Inc.).

Exhaust Valve Opening Time [CAD, ATDC]	151	156	161	166	171	176	
Intake valve opening time [CAD, ATDC]	322	2.60	1.91	1.43	1.12	0.95	0.90
	327	2.97	2.21	1.64	1.26	1.01	0.89
	332	3.40	2.59	1.96	1.49	1.17	0.98
	337	3.87	3.07	2.39	1.84	1.43	1.16
	342	4.37	3.62	2.94	2.35	1.85	1.48
	347	4.86	4.21	3.60	3.01	2.47	2.00
	352	5.29	4.80	4.31	3.81	3.30	2.80

The opening time of the intake valve was fixed to the maximum torque operating condition of 327 CAD ATDC in order to observe the change of performance according to the opening time of the exhaust valve. Moreover, the opening time of the exhaust valve changed. The results for the torque, intake airflow rate, and efficiency are shown in Figure 6. In general, when the exhaust valve opened ABDC, the exhaust gas was not completely discharged during the exhaust stroke because of the inertia of the combustion gas due to the movement of the piston. Therefore, the opening time of the exhaust valve was controlled before dead center of the bottom [28]. When the opening timing of the exhaust valve was retarded under the condition of a constant intake valve opening time, and when the amount of the exhaust remaining after opening the intake valve was increased due to the decreased blowdown duration and a hindered scavenging process, the intake airflow rate and torque decreased. However, the thermal efficiency increased, since the scavenging air/fuel mixture decreases during the valve

overlap [29]. On the other way, when the opening time of the exhaust valve advanced excessively, the effective work resulting from the blowdown and scavenging effect decreased due to the exhaust gas leaving the cylinder. The pressure drop during the earlier part of the expansion stroke significantly influences the decrease in expansion work [30]. As a result, the torque and efficiency decreased, as shown in the figure.

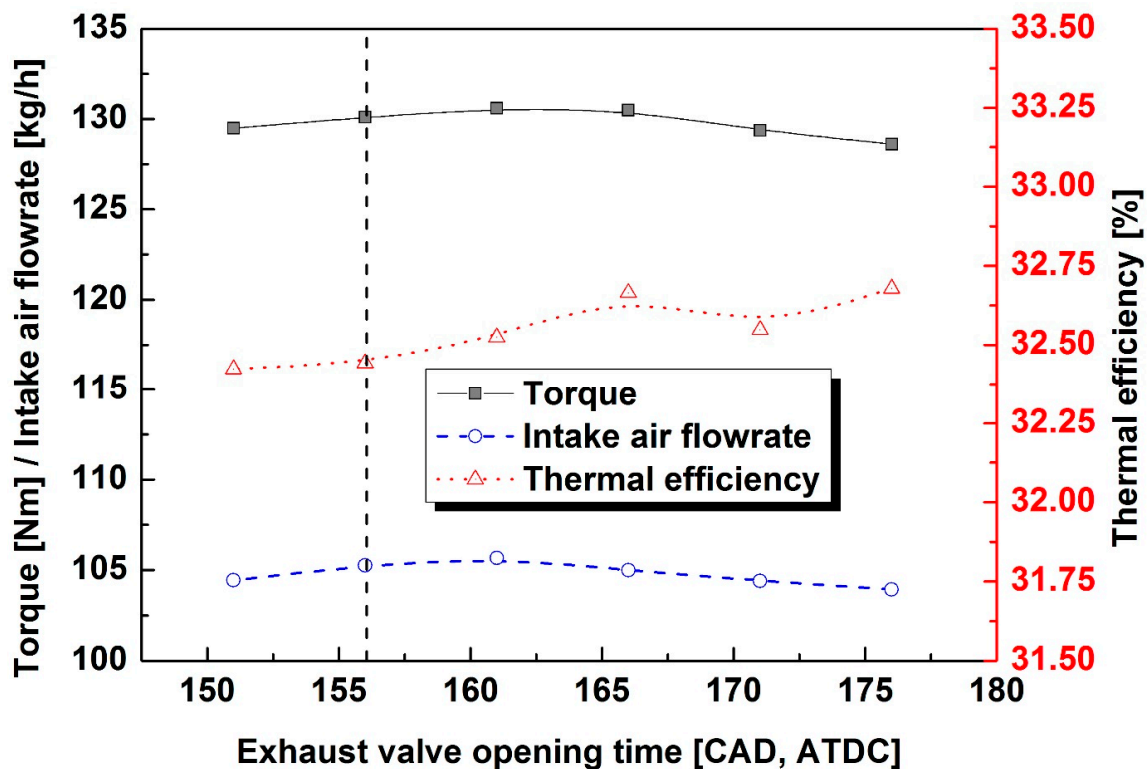


Figure 6. Torque, intake airflow rate, and thermal efficiency variations with exhaust valve opening time change at constant intake valve opening time of 327 CAD ATDC and excess air ratio of 1.25.

Figure 7 shows the characteristics of the excess air ratio when a richer mixture was supplied under the same operating conditions as those that are shown in Figure 6. Under most operating conditions, the ratio of the hydrogen fuel flow to the intake airflow rate was small, at approximately 2%. Therefore, a change in the airflow rate was not observed at the excess air ratio of 1.2, where the flow rate of the hydrogen fuel relatively increased. Similar to the results that are shown in Figure 3, the torque increased by the increased amount of fuel introduced in the mixture, while the efficiency decreased as the mixture became richer due to the reduced air utilization and the higher combustion temperature. However, the maximum torque value was confirmed at the exhaust valve opening time of 161 CAD ATDC without changing the tendency for the purpose of changing the exhaust valve opening time.

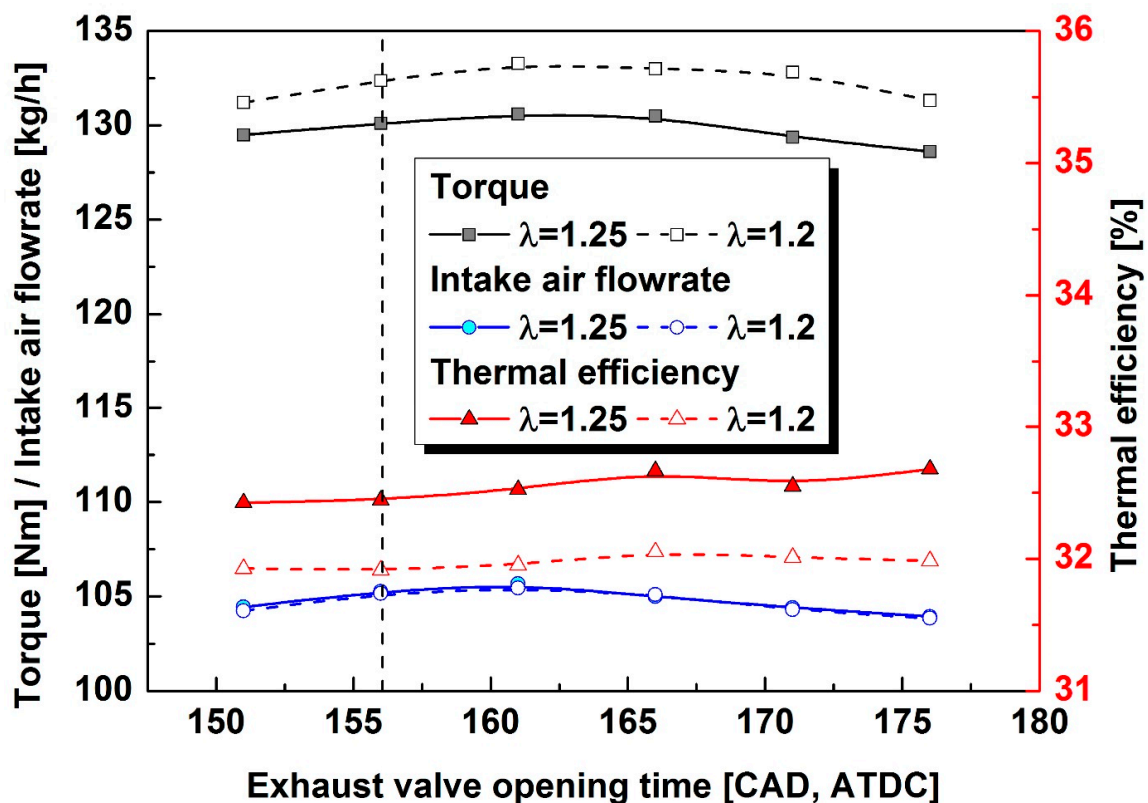


Figure 7. Torque, intake airflow rate, and thermal efficiency variations with exhaust valve open timing change at constant intake valve open timing of 327 CAD ATDC and excess air ratios of 1.25 and 1.20.

The opening time of the exhaust valve was fixed to 161 CAD ATDC and the results of the torque were observed with the excess air ratio and intake valve opening time variations in Figure 8, since the torque change with respect to the change of the opening time of the exhaust valve was not greater than that observed when the opening time of the intake valve was changed.

When the stable operation is secured at the lowest excess air ratio of 1.14, the highest torque of 138.1 Nm results was obtained at the intake valve opening time of the 327 CAD condition. Moreover, similar results were obtained under the 332 CAD conditions. However, under a condition that was more retarded than the 332 CAD condition, the torque decreased as the intake valve opening time was retarded. Because of backfire, it became impossible to operate the engine under a condition of a relatively richer mixture, as compared to the condition where the excess air ratio was 1.15. In the case of advancing to 327 CAD or less, the torque was similar to the result that was obtained at 332 CAD, since this did not significantly affect the intake air amount. However, if the intake valve opening time advanced excessively, as was the case under the 322 CAD condition, the combustion gas, which was hot and not exhausted from the cylinder, was in contact with the hydrogen-air mixture and it generated the high probability of a local combustion high. Therefore, it was more difficult to operate the engine with a richer mixture, as compared to the excess air ratio of 1.20. Even when the rich mix was fed with the addition of hydrogen fuel at a retarded intake valve opening time, the results indicated that the torque value was proportionally low to the advanced condition. However, even when the opening time of the intake and the exhaust valves were controlled, it was not possible to obtain a stable operating condition under which backfire would not occur with a relatively rich mixture condition near the excess air ratio of 1.1. Generally, torque and thermal efficiency are significantly influenced by the excess air ratio, but the changing intake valve opening time does not affect the thermal efficiency, as shown in Figure 9, since the variation of the total amount of hydrogen/air mixture scarcely influence the combustion speed at a certain excess air ratio condition.

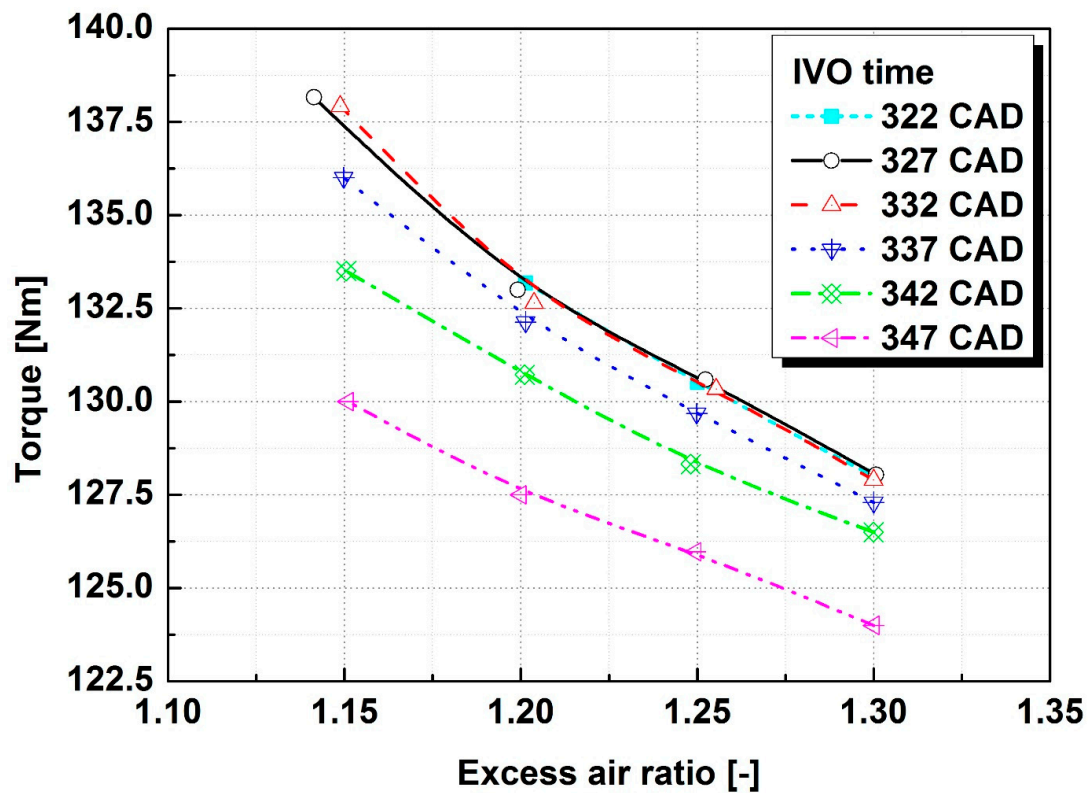


Figure 8. Torque changes with intake valve opening time and excess air ratio changes at constant exhaust valve opening time of 161 crank angle degree after top dead center (CAD ATDC).

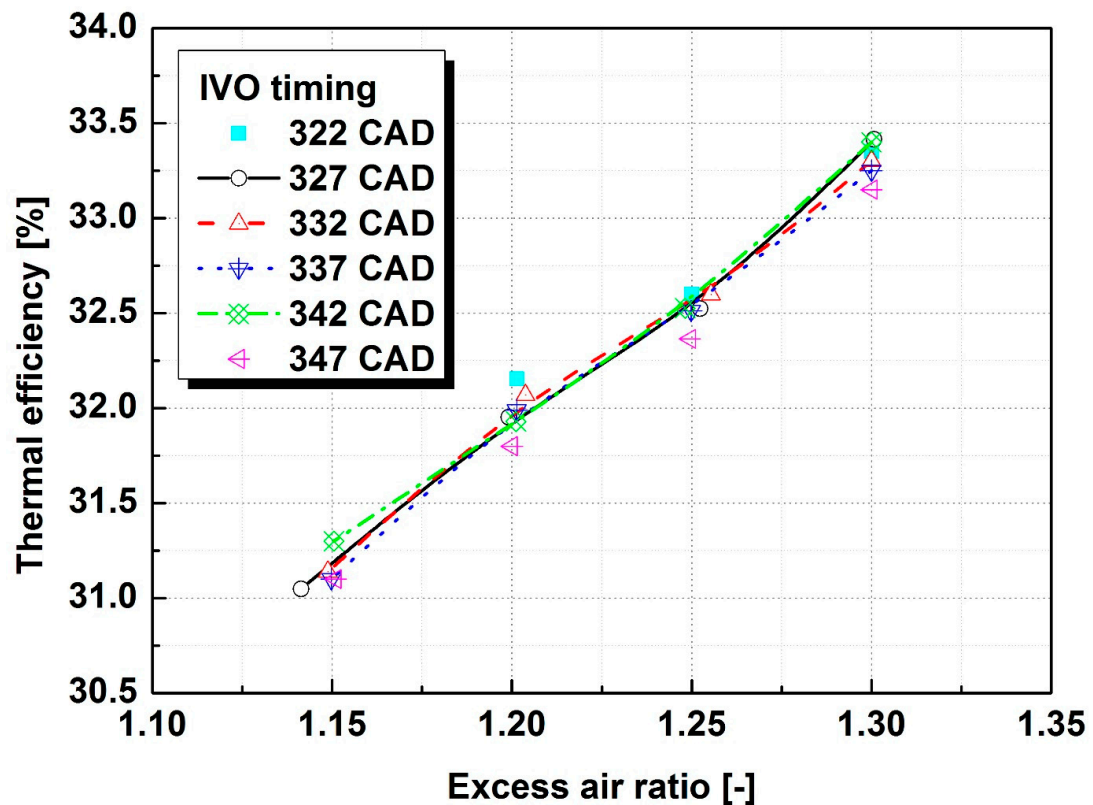


Figure 9. Thermal efficiency changes with intake valve opening time and excess air ratio changes at constant exhaust valve opening time of 161 CAD ATDC.

Figure 10 compares the equivalence ratios when the piston and valve movements were at 40 CAD ATDC and when the excess air ratio was 1.1 and 1.15, respectively. Although there was a difference in the local equivalence ratios, similar trends in the distribution of fuel have been confirmed in their entirety. Thereby, it was considered that the increase of a small amount of hydrogen fuel did not affect the occurrence of backfire. The temperature distributions in Kelvin are compared in Figure 11 under the same operating conditions and with the same timing as the conditions that are shown in Figure 10. The tendency of the overall temperature distribution was similar under both excess air ratio conditions. However, a higher temperature was observed in the combustion chamber wall, the intake valve portion of the exhaust valve, and the adjacent portion at the excess air ratio under the 1.1 condition, which was relatively rich. The reason for this is that there was no difference in the flow under the same valve opening time condition, although, under the rich mixture condition, the temperature of the exhaust gas increased after combustion. Additionally, the temperature of the remaining combustion gas in the combustion chamber increased to the temperature of the combustion chamber at the opening time of the intake valve. Consequently, it was considered that backfire occurred because of the temperature increase in the combustion chamber, rather than because of the effect of changing the fuel distribution under the rich mixture condition, where the other combustion control factors were constantly fixed and only the hydrogen fuel supply was increased.

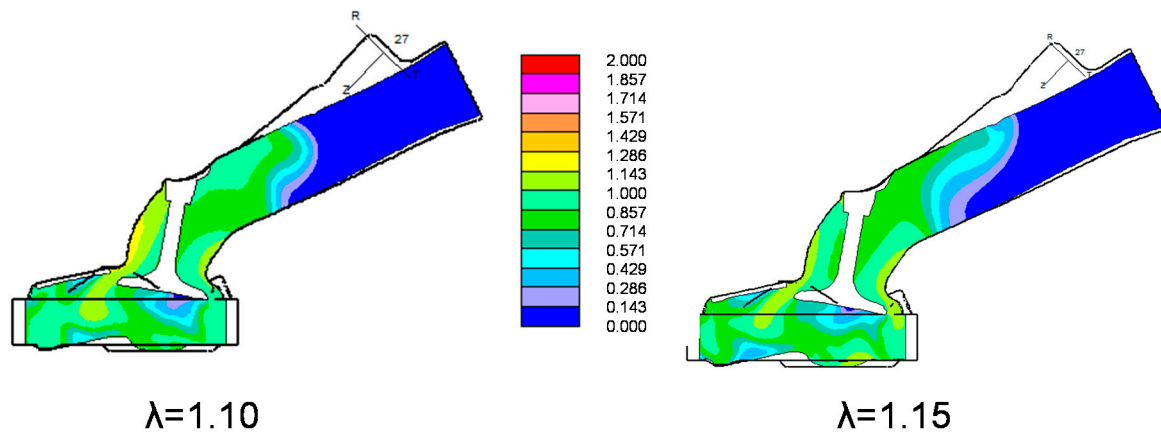


Figure 10. Simulated spatial distribution of equivalence ratios when piston and valve movements were at 40 CAD ATDC with excess air ratios of 1.1 and 1.15.

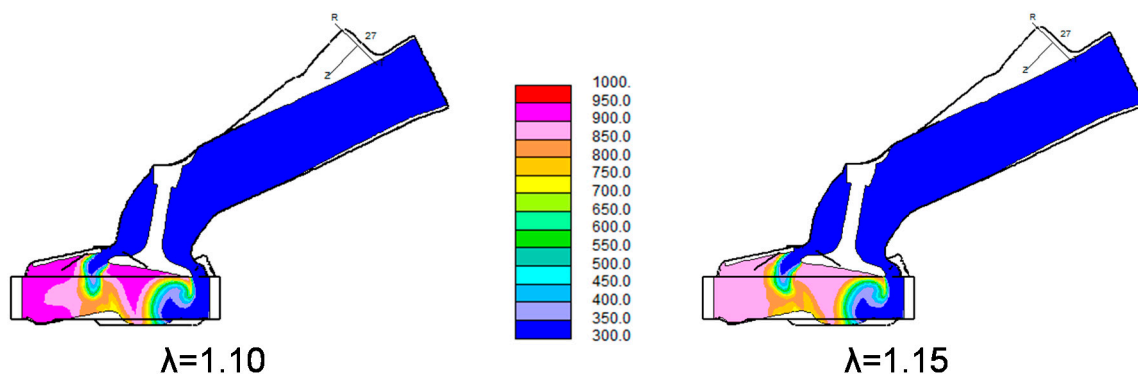


Figure 11. Simulated spatial distribution of temperature in Kelvin when piston and valve movements were at 40 CAD ATDC with excess air ratios of 1.1 and 1.15.

4. Conclusions

In this study, the combustion characteristics of a hydrogen engine for a HALE UAV were investigated under low engine speed and high load operating conditions. The intake and exhaust valve opening time and the excess air ratio of the mixture were optimized in order to achieve stable

combustion and to maximize torque. Using 3D CFD code in order to analyze the cause of the backfire in the hydrogen port fuel injection engine assessed the effect of the air excess ratio on the fuel and temperature distributions. The main results that were obtained from the intake and exhaust valve opening time change operations are summarized, as follows:

1. As the intake valve opening time advanced at a certain excess air ratio, the intake air amount and torque increased, and the intake airflow and torque were reduced, since the exhaust gas obstructed them and because the closing time of the intake valve was too quick.
2. When the opening time of the exhaust valve was retarded, the intake airflow rate and the torque decreased. However, the torque and thermal efficiency decreased when the opening time of the exhaust valve advanced excessively due to the increased pumping loss.
3. The change of the mixture's excess air ratio did not influence the tendency of the torque variation with the exhaust valve opening time. Moreover, the torque increased as the mixture became richer.
4. Under a condition that was more retarded than 332 CAD, the torque decreased when the intake valve opening time was retarded. Because of backfire, it was impossible to operate the engine under a richer mixture condition, as compared to the excess air ratio of 1.15.
5. The 3D CFD code simulation indicated that the backfire occurred because the temperature increased in the combustion chamber, rather than because of the effect of the change of fuel distribution under the rich mixture condition where the other combustion control factors were constantly fixed and only the hydrogen fuel supply was increased.

Author Contributions: C.P. and Y.K. conceived and designed the experiments; W.P. performed the simulation works of STAR-CD; C.P. and Y.C. analyzed the data; B.L. contributed reagents/materials/analysis tools; C.P. wrote the paper.

Funding: This research received no external funding.

Acknowledgments: This study was financially supported by Korea Aerospace Research Institute as a part of a project titled "Preliminary study on operation characteristics of hydrogen internal combustion engine with turbocharger." The authors sincerely appreciated the support.

Conflicts of Interest: The authors declare no conflict of interest.

References

1. Gundlach, J. Designing Unmanned Aircraft Systems: A Comprehensive Approach. *Aurora Flight Sci.* **2011**, *869*. [[CrossRef](#)]
2. Nickol, C.; Guynn, M.; Kohout, L.; Ozoroski, T. High Altitude Long Endurance Air Vehicle Analysis of Alternatives and Technology Requirements Development. In Proceedings of the 45th AIAA Aerospace Science Meeting and Exhibit, Reno, NV, USA, 8–11 January 2007.
3. Drell, I.L.; Belles, F.E. *Survey of Hydrogen Combustion Properties*; National Advisory Committee for Aeronautics: Washington, DC, USA, 1957.
4. Lewis, B.; Von Elbe, G. *Combustion, Flames, and Explosions of Gases*, 3rd ed.; Academic Press: Orlando, FL, USA, 1987; ISBN 978-0-12-446751-4.
5. Swain, M.R.; Pappas, J.M.; Adt, R.R.; Escher, W.J.D. *Hydrogen-Fueled Automotive Engine Experimental Testing to Provide an Initial Design-Data Base*; SAE Technical Paper; SAE International: Warrendale, PA, USA, 1981.
6. Das, L.M. Exhaust emission characterization of hydrogen-operated engine system: Nature of pollutants and their control techniques. *Int. J. Hydrogen Energy* **1991**, *16*, 765–775. [[CrossRef](#)]
7. Dunn, S. *Hydrogen Futures: Toward a Sustainable Energy System*; Worldwatch Institute: Washington, DC, USA, 2001; ISBN 978-1-878071-59-0.
8. Eichlseder, H.; Wallner, T.; Freymann, R.; Ringler, J. *The Potential of Hydrogen Internal Combustion Engines in a Future Mobility Scenario*; SAE Technical Paper; SAE International: Warrendale, PA, USA, 2003.
9. Berckmüller, M.; Rottengruber, H.; Eder, A.; Brehm, N.; Elsässer, G.; Müller-Alander, G.; Schwarz, C. *Potentials of a Charged SI-Hydrogen Engine*; SAE Technical Paper; SAE International: Warrendale, PA, USA, 2003.
10. Verhelst, S.; Sierens, R.; Verstraeten, S. *A Critical Review of Experimental Research on Hydrogen Fueled SI Engines*; SAE Technical Paper; SAE International: Warrendale, PA, USA, 2006.

11. White, C.M.; Steeper, R.R.; Lutz, A.E. The hydrogen-fueled internal combustion engine: A technical review. *Int. J. Hydrogen Energy* **2006**, *31*, 1292–1305. [[CrossRef](#)]
12. Verhelst, S.; Wallner, T. Hydrogen-fueled internal combustion engines. *Prog. Energy Combust. Sci.* **2009**, *35*, 490–527. [[CrossRef](#)]
13. Lim, G.; Lee, S.; Park, C.; Choi, Y.; Kim, C. Effect of ignition timing retard strategy on NO_x reduction in hydrogen-compressed natural gas blend engine with increased compression ratio. *Int. J. Hydrogen Energy* **2014**, *39*, 2399–2408. [[CrossRef](#)]
14. DeLuchi, M.A. Hydrogen vehicles: an evaluation of fuel storage, performance, safety, environmental impacts, and cost. *Int. J. Hydrogen Energy* **1989**, *14*, 81–130. [[CrossRef](#)]
15. Tang, X.; Kabat, D.M.; Natkin, R.J.; Stockhausen, W.F.; Heffel, J. *Ford P2000 Hydrogen Engine Dynamometer Development*; SAE Technical Paper; SAE International: Warrendale, PA, USA, 2002.
16. Rottengruber, H.; Berckmüller, M.; Elsässer, G.; Brehm, N.; Schwarz, C. *Direct-Injection Hydrogen SI-Engine-Operation Strategy and Power Density Potentials*; SAE Technical Paper; SAE International: Warrendale, PA, USA, 2004.
17. Huynh, T.C.; Kang, J.K.; Noh, K.C.; Lee, J.T.; Caton, J.A. Controlling Backfire for a Hydrogen-Fueled Engine Using External Mixture Injection. *J. Eng. Gas Turbines Power* **2008**, *130*, 062804. [[CrossRef](#)]
18. Karim, G.A. Hydrogen as a spark ignition engine fuel. *Int. J. Hydrogen Energy* **2003**, *28*, 569–577. [[CrossRef](#)]
19. Heywood, J.B. *Internal Combustion Engine Fundamentals*; McGraw-Hill: New York, NY, USA, 1988; ISBN 0-07-028637-X, 978-0-07-028637-5, 0-07-100499-8, 978-0-07-100499-2.
20. Stone, R. *Introduction to Internal Combustion Engines*; Palgrave Macmillan: Basingstoke, UK, 2012; ISBN 978-0-230-57663-6, 0-230-57663-X.
21. Duan, J.; Liu, F.; Sun, B. Backfire control and power enhancement of a hydrogen internal combustion engine. *Int. J. Hydrogen Energy* **2014**, *39*, 4581–4589. [[CrossRef](#)]
22. Liu, X.; Liu, F.; Zhou, L.; Sun, B.; Schock, H.J. Backfire prediction in a manifold injection hydrogen internal combustion engine. *Int. J. Hydrogen Energy* **2008**, *33*, 3847–3855. [[CrossRef](#)]
23. Yousufuddin, S.; Masood, M. Effect of ignition timing and compression ratio on the performance of a hydrogen-ethanol fuelled engine. *Int. J. Hydrogen Energy* **2009**, *34*, 6945–6950. [[CrossRef](#)]
24. Yakhot, V.; Orszag, S.A. Renormalization group analysis of turbulence. I. Basic theory. *J. Sci. Comput.* **1986**, *1*, 3–51. [[CrossRef](#)]
25. Kukkonen, C.A.; Shelef, M. *Hydrogen as an Alternative Automotive Fuel: 1993 Update*; SAE International: Warrendale, PA, USA, 1994.
26. Myung, C.L.; Choi, K.H.; Hwang, I.G.; Lee, K.H.; Park, S. Effects of valve timing and intake flow motion control on combustion and time-resolved HC & NO_x formation characteristics. *Int. J. Automot. Technol.* **2009**, *10*, 161–166.
27. Choi, K.; Lee, H.; Hwang, I.G.; Myung, C.-L.; Park, S. Effects of various intake valve timings and spark timings on combustion, cyclic THC and NO_x emissions during cold start phase with idle operation in CVVT engine. *J. Mech. Sci. Technol.* **2009**, *22*, 2254–2262. [[CrossRef](#)]
28. Roberts, L.E. Analysis of the Impact of Early Exhaust Valve Opening and Cylinder Deactivation on Aftertreatment Thermal Management and Efficiency for Compression Ignition Engines. Master's Thesis, Purdue University, West Lafayette, IN, USA, 2014.
29. Wang, X.; Ma, J.; Zhao, H. Analysis of scavenge port designs and exhaust valve profiles on the in-cylinder flow and scavenging performance in a two-stroke boosted uniflow scavenged direct injection gasoline engine. *Int. J. Engine Res.* **2018**, *19*, 509–527. [[CrossRef](#)]
30. Bharath, A.N.; Kalva, N.; Reitz, R.D.; Rutland, C.J. Use of Early Exhaust Valve Opening to Improve Combustion Efficiency and Catalyst Effectiveness in a Multi-Cylinder RCCI Engine System: A Simulation Study. In Proceedings of the ASME 2014 Internal Combustion Engine Division Fall Technical Conference Volume 1: Large Bore Engines, Fuels, Advanced Combustion, Emissions Control Systems, Columbus, IN, USA, 19–22 October 2014.

